THE JOURNAL OF BIOLOGICAL CHEMISTRY
Vol. 275, No. 4, Issue of January 28, pp. 2745–2755, 2000

Printed in U.S.A.

A Developmentally Regulated Aconitase Related to Iron-regulatory Protein-1 Is Localized in the Cytoplasm and in the Mitochondrion of *Trypanosoma brucei**

(Received for publication, October 6, 1999)

Joachim Saas‡§, Karl Ziegelbauer¶‖, Arndt von Haeseler, Beate Fast‡§, and Michael Boshart‡§‡‡**

*From the ‡Arbeitsgruppe Molekulare Zellbiologie, Institut für Molekularbiologie und Biochemie und Institut für Infektionsmedizin, Freie Universität, Berlin, the §Max-Planck-Institut für Biochemie, Martinsried, the ¶Max-Planck-Institut für Biologie, Tübingen, and the **Max-Planck-Institut für Evolutionäre Anthropologie, Leipzig, Germany*

Mitochondrial energy metabolism and Krebs cycle activities are developmentally regulated in the life cycle of the protozoan parasite *Trypanosoma brucei*. Here we report cloning of a *T. brucei* aconitase gene that is closely related to mammalian iron-regulatory protein 1 (IRP-1) and plant aconitases. Kinetic analysis of purified recombinant TbACO expressed in *Escherichia coli* resulted in a K_m (isocitrate) of 3 ± 0.4 mM, similar to aconitases of other organisms. This was unexpected since an arginine conserved in the aconitase protein family and crucial for substrate positioning in the catalytic center and for activity of pig mitochondrial aconitase (Zheng, L., Kennedy, M. C., Beinert, H., and Zalkin, H. (1992) *J. Biol. Chem.* 267, 7895–7903) is substituted by leucine in the TbACO sequence. Expression of the 98-kDa TbACO was shown to be lowest in the slender bloodstream stage of the parasite, 8-fold elevated in the stumpy stage, and increased a further 4-fold in the procyclic stage. The differential expression of TbACO protein contrasted with only minor changes in *TbACO* mRNA, indicating translational or post-translational mechanisms of regulation. Whereas animal cells express two distinct compartmentalized aconitases, mitochondrial aconitase and cytoplasmic aconitase/IRP-1, TbACO accounts for total aconitase activity in trypanosomes. By cell fractionation and immunofluorescence microscopy, we show that native as well as a transfected epitope-tagged TbACO localizes in both the mitochondrion (30%) and in the cytoplasm (70%). Together with phylogenetic reconstructions of the aconitase family, this suggests that animal IRPs have evolved from a multicompartmentalized ancestral aconitase. The possible functions of a cytoplasmic aconitase in trypanosomes are discussed.

Trypanosoma brucei is a protozoan parasite in the blood and tissue fluids of mammals and causes two major tropical diseases, sleeping sickness in man and nagana in cattle. The flagellate is transmitted in subsaharan Africa between humans, livestock, and a huge reservoir of game animals by the tsetse fly, a bloodsucking insect vector. During cyclical transmission between mammals and tsetse, trypanosomes differentiate into a series of life cycle stages with distinct morphology, metabolism, and surface proteins to cope with the changing host environments and host defense mechanisms (1). The proliferating forms in the host blood have elongated and slender appearance (long slender forms) and rely entirely on glycolysis for energy production (2–4). Inefficient substrate utilization seems affordable at that developmental stage, due to glucose homeostasis in host blood. Hence, slender forms lack significant amounts of Krebs cycle enzymes (5), and their residual mitochondrion does not contribute to ATP production. At the peak of a parasitemic wave, slender forms differentiate into a quiescent, cell cycle-arrested stage with stumpy morphology (stumpy form) which has a more developed mitochondrion and expresses citric acid cycle activities and an incomplete electron transport chain (5–8). In culture, differentiation to the stumpy stage is induced by a cell density sensing mechanism acting via the cAMP second messenger pathway (9, 10). A population of stumpy forms, in turn, can be triggered to differentiate rapidly and synchronously to the next stage in the life cycle, the procyclic forms, which populate the fly midgut and rely on respiration of proline as their major energy source. Therefore, induction of Krebs cycle enzymes and of a respiratory chain in stumpy forms is regarded as a preadaptation to the fly environment (8). The signal for differentiation to procyclic forms in the midgut of the tsetse is unknown; however, the process can be triggered in culture by a temperature shift to 27 °C or most efficiently by addition of *cis*-aconitate or citrate to the culture medium (11, 12). The differentiation inducing effect of *cis*-aconitate and citrate is highly specific. The peculiar role of these substrates in triggering a developmental switch and the coordinate induction of the citric acid cycle enzymes during differentiation to the stumpy stage prompted us to identify and characterize the aconitase gene of *T. brucei*.

Aconitase (citrate(isocitrate) hydro-lyase, EC 4.2.1.3) catalyzes the stereospecific dehydration/rehydration reaction of citrate to isocitrate via the intermediate *cis*-aconitate (13). Activity of the enzyme critically depends on the presence of an iron sulfur [4Fe4S] cluster in the catalytic center that is highly sensitive to oxygen. Upon oxidation the cluster is converted to an inactive [3Fe4S] form (14). Mammalian cells express two distinct aconitases encoded by separate genes: (*a*) mitochondrial aconitase and (*b*) a bifunctional cytoplasmic aconitase

* This work was supported by Bundesministerium für Bildung, Wissenschaft, und Forschung Grant 0311092 (to M. B.). The costs of publication of this article were defrayed in part by the payment of page charges. This article must therefore be hereby marked "*advertisement*" in accordance with 18 U.S.C. Section 1734 solely to indicate this fact.

The nucleotide sequence(s) reported in this paper has been submitted to the GenBank™/EBI Data Bank with accession number(s) AF127456, AF127457, and AF190556.

‖ Present address: Bayer Yakuhin Ltd., Research Center Kyoto, 6-5-1-3 Kunimidai, Kizu-cho, Soraku-gun, Kyoto, 619-02, Japan.

‡‡ To whom correspondence should be addressed: AG Molekulare Zellbiologie, Institut für Molekularbiologie und Biochemie, FU Berlin, Hindenburgdamm 27, D-12203 Berlin, Germany. Tel.: 49-30-8445-3820; Fax: 49-30-8445-3840; E-mail: boshart@ukbf.fu-berlin.de.

that is identical to the iron-regulatory protein (IRP-1).[1] IRP-1 is an RNA-binding protein interacting with iron-responsive elements (IREs) in the untranslated regions of several mRNAs (15), including the transferrin receptor and ferritin H- and L-subunits (16), and functions in coordinate post-transcriptional regulation of cellular iron metabolism (17, 18). In iron-loaded cells, IRP-1 assembles a cubane [4Fe-4S] cluster, which renders it active as a cytosolic aconitase but inactive for RNA binding. Disassembly of the cluster upon iron starvation yields the active RNA-binding form that regulates stability or translation of target RNAs. The two conformations and functional states are mutually exclusive. Cytoplasmic aconitase activity might also be required for a glyoxalate cycle in specialized animal tissues like brown adipose tissue (19). In plants, where cytoplasmic aconitase is developmentally regulated and abundant in germinating seeds, its role in the glyoxalate cycle is well established (20, 21).

Here we report on cloning and characterization of a protozoan aconitase that is closely related to animal IRPs and plant aconitases. Dual subcellular localization of the developmentally regulated *T. brucei* enzyme suggests that it not only takes part in the mitochondrial Krebs cycle but may have a yet unknown function in the cytoplasm of the parasite.

EXPERIMENTAL PROCEDURES

Trypanosomes, Cell Culture, and Transfection—Bloodstream forms of the pleomorphic *T. brucei brucei* clone AnTat1.1 were grown in rodents as described (22). The monomorphic clone MiTat1.4 (23) was cultured in HMI-9 medium (24) supplemented with 10% (v/v) heat-inactivated fetal bovine serum but without Serum Plus™ at 37 °C and 5% (v/v) CO_2. Procyclic forms were cultured at 27 °C in SDM-79 (25) supplemented with 10% (v/v) heat-inactivated fetal bovine serum. Bloodstream forms were purified from host blood by ion exchange chromatography (26) on DEAE-Sephacel (Amersham Pharmacia Biotech) columns. For stable transfection, 10 μg of *Not*I-linearized plasmid DNA was electroporated (BTX 600 Electro Cell Manipulator, 1.2 kV, 25 microfarads, 186 ohms, 2-mm electrode distance) into 4×10^7 MiTat1.4 bloodstream forms in a volume of 0.5 ml (27). After 24 h, cells were selected with 0.5 μg/ml phleomycin, and after several passages, drug-resistant pools were differentiated *in vitro* into procyclic forms as described before (22).

Genomic Cloning—The consensus motifs IGTDSHT and NM(C/G)(A/P)E(I/Y)GA from the first and second domain of aconitases and IRPs of several species (*underlined* in Fig. 3) were selected to design pools of degenerate primers as follows: sense primer 5′ ATHGGNACNGAYTCNCAYAC 3′ (768-fold degenerated) and antisense primer 5′ GCNCCRTAYTCNGSRCMCATRTT 3′ (1024-fold degenerated) were used to amplify 1 μg of genomic AnTat1.1 DNA (30 cycles, 1.5 min 94 °C, 2 min 45 °C, and 2 min 72 °C) using *Pfu* polymerase (Stratagene). Products of expected size (300 bp) were cloned into a *Sma*I-linearized pBluescriptSKII(+) vector and transformed into *Escherichia coli* XL-1 Blue MRA (Stratagene). Genomic *T. brucei* DNA was cut with *Sac*II and *Pst*I and separated on a preparative 0.8% (w/v) agarose gel, and individual size fractions in the range of 3–4 kb were eluted. The fraction containing the 3.6-kb *Sac*II-*Pst*I fragment (Fig. 2) was identified by Southern blotting and was used to construct a library in plasmid pBluescriptSKII(+) cut with *Sac*II and *Pst*I which was transformed into *E. coli* DH5α. Tbaco1.1 (Fig. 2) was isolated by two rounds of bacterial colony screening with the 311-bp *TbACO* fragment as probe. For inverted PCR of the 3′-end of TbACO, genomic *T. brucei* AnTat1.1 DNA was digested with *Sac*II and separated on a preparative 0.8% (w/v) agarose gel, and the size fraction between 5 and 7.5 kb in size was isolated and circularized with T4 DNA ligase. For amplification, the nested primer pairs 5′ CGGGCAAGATACTCAAGGTTCACT 3′ (JS/5.4) plus 5′ GGCGACTCCATAACCACAGACCAT 3′ (IRP.4) and 5′ CTCTTGTGGCAGTTCTCGC 3′ (JS5–2) plus 5′ ACGGCTCTTCCTTCAGTG 3′ (IRP.1) were used.

cDNA Cloning—For 5′-RACE, 20 μg of total RNA isolated from procyclic forms of AnTat1.1 were reversely transcribed with the *TbACO* sequence-specific oligonucleotide 5′ GGGAACGCCAGTGAAGTC 3′ (JS5–1) and Superscript™ Reverse Transcriptase (Life Technologies, Inc.). After RNA hydrolysis the cDNA was PCR-amplified with a primer matching the spliced leader sequence of *T. brucei*, 5′ GGGAATTCCGCTATTATTAGAACAGTTTCT 3′ (where underlines indicate restriction sites) and the nested *TbACO*-specific primer JS5-2 (see above). The resulting PCR fragment was digested with *Eco*RI and *Eco*RV and cloned into pBluescriptSKII(+) cut with *Eco*RI and *Hinc*II. For cDNA cloning of the 3′-end of the gene, reverse transcription was primed with a *Xho*I/*Sal*I/*Cla*I $d(T)_{17}$ primer (5′ GACTCGAGTCGACATCGAT$_{17}$ 3′) followed by PCR with the adaptor primer 5′ GACTCGAGTCGACATCG 3′ and the *TbACO*-specific nested primers 5′ ATGGCAGGAATCCACATA 3′ (RIRP-2) and 5′ TGCCAACACCCGACTTG 3′ (RIRP-1) or with adaptor primer and primer 5′ GGGAACTATGTGTGATGAGG 3′ (IRP.6).

DNA Sequencing—The sequence of the antisense strand was determined from overlapping deletion clones of plasmid Tbaco1.1, constructed as recommended by the supplier of the Nested Deletion Kit (Amersham Pharmacia Biotech). The nucleotide sequences of the sense strand, of cDNA clones, and of the genomic clone obtained by inverted PCR were determined by primer walking. The Sequenase™ version 2.0 Sequencing Kit (U. S. Biochemical Corp.) and a fluorescent dideoxynucleotide terminator cycle sequencing kit (Applied Biosystems) were used for manual and automated sequencing, respectively.

Plasmid Constructs and Site-directed Mutagenesis—The complete coding region of *TbACO* was assembled from a 104-bp *Pst*I-*Eco*RV fragment derived from a 3′-RACE clone and the genomic clone Tbaco1.1 opened with *Pst*I (partial digest) and *Xba*I (blunted). For convenient cloning, a *TbACO* cassette was constructed as follows: a *Bam*HI site was introduced immediately upstream of the start codon by recombinant PCR using the primers 5′ CGGGATCCATGCTCAGCACGATGAAG 3′ and JS5-2 (see cDNA cloning), and a *Bgl*II site was introduced exactly after the stop codon with the primers RIRP-2 (see cDNA cloning) and 5′ GAAGATCTCTACAAATTACCCTTGATT 3′. The cassette was then recloned between *Bam*HI and *Sal*I of BluescriptSKII(−). Details of these constructions are available upon request.

For bacterial expression, the following *TbACO* fragments were cloned into the hexahistidine tag expression vector pQE30 (Qiagen): a *Stu*I-*Pst*I fragment of Tbaco1.1 resulting in pQE31/13 (88 kDa), a *Bam*HI-*Pst*I fragment of Tbaco1.1 resulting in pQE30/4 (90 kDa), and the full-length *TbACO* cassette excised with *Bam*HI and *Sal*I resulting in pQE30/5 (99 kDa). A Cys-446 → Ser point mutation and a Cys-512 → Ser/Cys-515 → Ser double point mutation were introduced into TbACO using the Transformer™ Site-directed Mutagenesis Kit (CLONTECH). To this end, a 302-bp *Apa*I-*Sma*I fragment of plasmid Tbaco1.1 was subcloned into pBluescriptSKII(−), and the mutagenesis was performed using the mutation primer MP1 5′ GCTATTACTTCCTCTACAAACACCTCG 3′ and the selection primer Sp1 5′ GTGACTGGTGAATACTCAACCAAG 3′. For the double mutant, a *Sma*I/*Sal*I 1273-bp fragment of pQE30/5 was subcloned into pBluescriptSKII(−), and the mutation primer MP2 5′ CGGGGTACGGCAGCATGACAAGCATCGGGAATG 3′ and the selection primer Sp1 were used (nucleotide mismatches are underlined). The mutagenized fragments were verified by sequencing and were cloned into pQE30/5 in exchange to the respective wild type fragments.

For expression of C-terminally tagged TbACO in trypanosomes, the insertion vector pLew20 which targets the rDNA spacer of *T. brucei* (28) was opened with *Hin*dIII and *Bam*HI; the ends were blunted, and the vector fragment was gel-purified. The Ty-1 epitope (29) was attached to the C terminus of TbACO by recombinant PCR using the *TbACO*-specific primer 5′ ATGGCAGGAATCCACATA 3′ and the Ty-1 primer 5′ GCTCTAGACTAGTCAAGTGGATCCTGGTTAGTATGGACCTCCAAATTACCCTTGATTTTC 3′ including an *Xba*I site. The resulting PCR fragment was cleaved with *Xba*I, blunted, and then cleaved with *Eco*47III. The *TbACO* cassette was cut with *Bam*HI, blunted, and then cut with *Eco*47III, followed by isolation of the fragment. The three fragments were ligated together to give pLewacotag.

Southern Blot Analysis—Genomic DNA was prepared by phenol extraction, dialysis, and isopropyl alcohol precipitation. After electrophoresis in TAE buffer, agarose gels were blotted onto a GeneScreen™ nylon membrane (NEN Life Science Products) by capillary transfer. The hybridization and washing temperatures were adjusted to 5 °C below the calculated melting temperature of specific DNA-DNA hybrids for high stringency conditions and to 40 °C below the calculated melting

[1] The abbreviations used are: IRP, iron-regulatory protein; IPTG, isopropyl-1-thio-β-D-galactopyranoside; IRE, iron-responsive element; kb, kilobase pairs; MES, 2-(*N*-morpholino)-ethanesulfonic acid; NBT, nitro blue tetrazolium; PCF, procyclic forms; PCR, polymerase chain reaction; SS, short stumpy forms; UTR, untranslated region; bp, base pair; DTT, dithiothreitol; PAGE, polyacrylamide gel electrophoresis; PBS, phosphate-buffered saline; RACE, rapid amplification of cDNA ends; NTA, nitrilotriacetic acid.

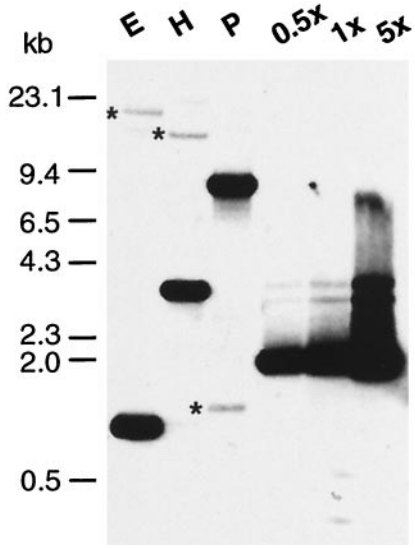

FIG. 1. ***TbACO* copy number and related sequences in the *T. brucei* genome.** Genomic *T. brucei* AnTat1.1 DNA was digested with *Eco*RI (*E*), *Hin*dIII (*H*), or *Pst*I (*P*), and 5 μg were loaded per lane on a 0.8% (w/v) agarose gel. Dilutions of a cloned *TbACO* fragment were loaded as sensitivity markers equivalent to 0.5, 1, and 5 copies per haploid genome (0.5, 1, and 5×). The Southern blot was probed with the 311-bp PCR fragment (see Fig. 2) labeled with [α-^{32}P]NTPs by primer extension. One additional weakly cross-hybridizing sequence (bands marked with an *asterisk*) was detected at low hybridization stringency (40 °C below the calculated melting point (T_m) of the probe) but not at stringent conditions (5 °C below T_m, not shown).

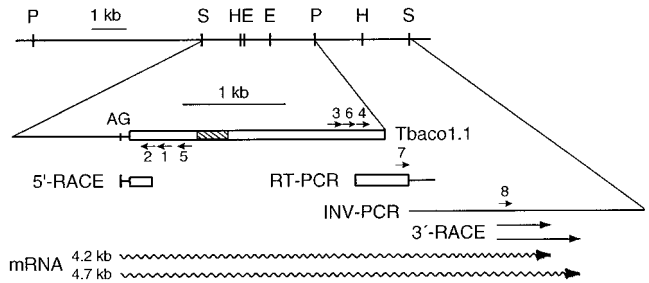

FIG. 2. **Restriction map of the *TbACO* locus and cloning strategy.** Genomic cleavage sites of *Eco*RI (*E*), *Hin*dIII (*H*), *Pst*I (*P*), and *Sac*II (*S*) are indicated for strain AnTat1.1 of *T. brucei*. The blow up represents the genomic *Sac*II-*Pst*I fragment (clone Tbaco1.1, GenBank™ accession number AF127456) that was isolated by screening with the 311-bp PCR fragment indicated by a *hatched box*. The TbACO open reading frame is *boxed*. The cDNA at the 3′-end (reverse transcriptase-PCR, GenBank™ accession number AF127457) was amplified with nested gene-specific primers RIRP2 (3) and RIRP1 (4). Four independent cDNA clones contributed 75 amino acids of coding region (*boxed*) as well as 254 bp of 3′-UTR. The *trans*-splice site (marked by an AG dinucleotide) at position −100 relative to the first ATG was determined from the sequence of 3 independent 5′-RACE clones amplified with nested gene-specific primers JS5-1 (1) and JS5-2 (2). The 3′-end of the gene was cloned by inverted PCR (*INV-PCR*, GenBank™ accession number AF190556) using the nested primer pairs JS/5.4 (5) plus IRP.4 (6) and JS5-2 (2) plus IRP.1 (7). The 3′-ends of *TbACO* transcripts (*wavy lines*) were mapped by 3′-RACE PCR using the gene-specific primer IRP.6 (8). Two PCR products of 500 and 810 bp (indicated by *arrows*) were obtained, thus calculated sizes of *TbACO* mRNAs (without poly(A)-tail) of 4197 and 4507 nt, respectively. The transcript sizes estimated from Northern blots (see Fig. 6) are indicated (4.2 and 4.7 kb).

temperature for low stringency conditions, using the buffers described in Boshart *et al.* (30). A *TbACO*-specific probe of defined length (nucleotides 1778–2088 of Tbaco1.1) was generated by primer extension (31) with polylinker-specific primers (SK and KS) using as template an *Eag*I- and *Apa*I-cut pBluescript plasmid containing the 311-bp PCR fragment.

Northern Blot Analysis—Total RNA was isolated using the guanidinium isothiocyanate/$CsCl_2$ cushion method (32) and was fractionated on 1.2% (w/v) formaldehyde-agarose gels and blotted onto GeneScreen™ (NEN Life Science Products) nylon membrane. A riboprobe corresponding to nucleotides 1778–2088 of Tbaco1.1 was prepared and hybridized as described (30)· The blot was washed three times for 30 min in 0.1× SSC, 1% (w/v) SDS at 65 °C. For control, the same blot was probed with the random prime-labeled plasmid pR4 containing part of the rRNA locus (33)·

Bacterial Expression of TbACO—E. coli M15rep4 (34) transformed with pQE30/5 was grown in LB medium containing 100 μg/ml ampicillin and 25 μg/ml kanamycin up to an A_{600} of 0.7, and TbACO expression was induced by addition of 1 mM IPTG for 3 h at 25 °C. Bacteria were freeze/thaw lysed and sonicated in 50 mM $Na_xH_yPO_4$ buffer, 300 mM NaCl, pH 8.0, 40 μg/ml bestatin, 1 μg/ml leupeptin, 0.5 μg/ml Pefabloc® (Roche Molecular Biochemicals) and 0.7 μg/ml pepstatin. The soluble material was purified by metal chelate affinity chromatography on a Ni^{2+}-NTA column (Qiagen) according to the manufacturer's protocols. The yield was in the range of 230 μg of soluble protein from 1 liter of culture. For further purification, this protein was dialyzed against 20 mM Tris-HCl, pH 7.5, 5% (v/v) glycerol and subjected to ion exchange chromatography on a MonoQ HR 5/5 column (Amersham Pharmacia Biotech). The N terminus of the recombinant protein was verified by microsequencing; an amino acid analysis gave results compatible with the predicted sequence of recombinant TbACO, and a mass spectrum gave a value of 99902.5 mass units compared with a theoretical value of 99702.7 (all performed by the protein chemistry core facility of the MPI for Biochemistry).

Enzyme Assays—For aconitase activity measurements, recombinant full-length TbACO (99 kDa) was expressed and purified as described above, except that all buffers contained 10 mM citrate and 2 mM β-mercaptoethanol and were degassed and saturated with nitrogen. The aconitase substrate citrate protects from oxidative inactivation (35). For concentration and buffer exchange (50 mM Tris-HCl, pH 7.5, 200 mM NaCl, 10 mM citrate, 1 mM DTT), Centricon™ 100 ultrafiltration units (Amicon) were used. Protein samples were stored in a glove bag under argon or nitrogen atmosphere at 4 °C. Iron loading under reducing conditions was performed in a glove bag with 200 μg of protein (in 20 mM Tris-HCl, pH 7.5) by adding 10× loading buffer (10 mM MES, pH 5.5, 10 mM ferrous ethylenediammonium sulfate, 50 mM DTT) and incubating for 25 min at 37 °C similar as described by Kennedy *et al.* (36). The loaded protein was aliquoted and stored on ice in nitrogen atmosphere until measurement of activity with a double beam photometer (Perkin-Elmer Lambda 5). For the UV assay described by Henson and Cleland (37), 1 ml of 90 mM Tris-HCl, pH 7.5, containing DL-isocitrate (Sigma) ranging from 1 to 20 mM was equilibrated at 25 °C, and the formation of *cis*-aconitate was recorded for 6 min (extinction coefficient for *cis*-aconitate ϵ = 3.4 mM^{-1} cm^{-1} at 240 nm). Assuming Michaelis-Menten kinetics, nonlinear curve fitting of kinetic data was performed with Kaleidagraph 3.0.8 (Synergy Software) and the K_m and V_{max} values were calculated from a reciprocal plot according to Hanes (38). Aconitase activity in whole cell extracts was measured as described by Overath *et al.* (7). Protein concentrations were determined using the Bradford assay as supplied by Bio-Rad and bovine serum albumin as standard.

Antibodies—For the first series of immunizations (including "rat 1"), an 88-kDa recombinant TbACO fragment (pQE31/13) was purified by Ni^{2+}-NTA chromatography, electrophoresed on an 8% (w/v) SDS-polyacrylamide gel, and blotted onto nitrocellulose membrane. The 88-kDa band was excised from the membrane (150–200 μg of protein), and the dried nitrocellulose was powdered, emulsified with complete Freund adjuvant, and injected intraperitoneally in female Wistar rats. Rats were boostered once with 150 μg of protein after 4 weeks. Two weeks later, the animals were bled, and sera were affinity purified as described (39). For a second series of immunizations (including "rat 2" and "rabbit 1") the recombinant full-length TbACO (pQE30/5) was purified by Ni^{2+}-NTA chromatography in soluble form and directly emulsified with complete Freund adjuvant. Rabbits were immunized by subdermal injection of 500 μg of protein followed by 3 booster injections at regular intervals. Rabbit anti-phosphoglycerate kinase C antibodies were a kind gift of P. Michels. Rabbit anti-*Synechococcus* sp. HSP60 antiserum was purchased from StressGen Biotechnologies Corp. The BB2 hybridoma (anti-Ty1 monoclonal antibody) was a kind gift of P. Bastin and K. Gull. Rabbit anti-*Dictyostelium* α-tubulin antiserum was obtained from G. Gerisch.

Immunoblot Analysis—Whole cell extracts were prepared by transferring small volumes of PBS-washed and resuspended trypanosomes into SDS-lysis buffer preheated to 100 °C. Samples were boiled for 5 min and sonified. Proteins were separated on 8% (w/v) SDS-polyacrylamide gels and were transferred onto Hybond™ polyvinylidene difluoride membranes (Amersham Pharmacia Biotech) using a semi-dry blot-

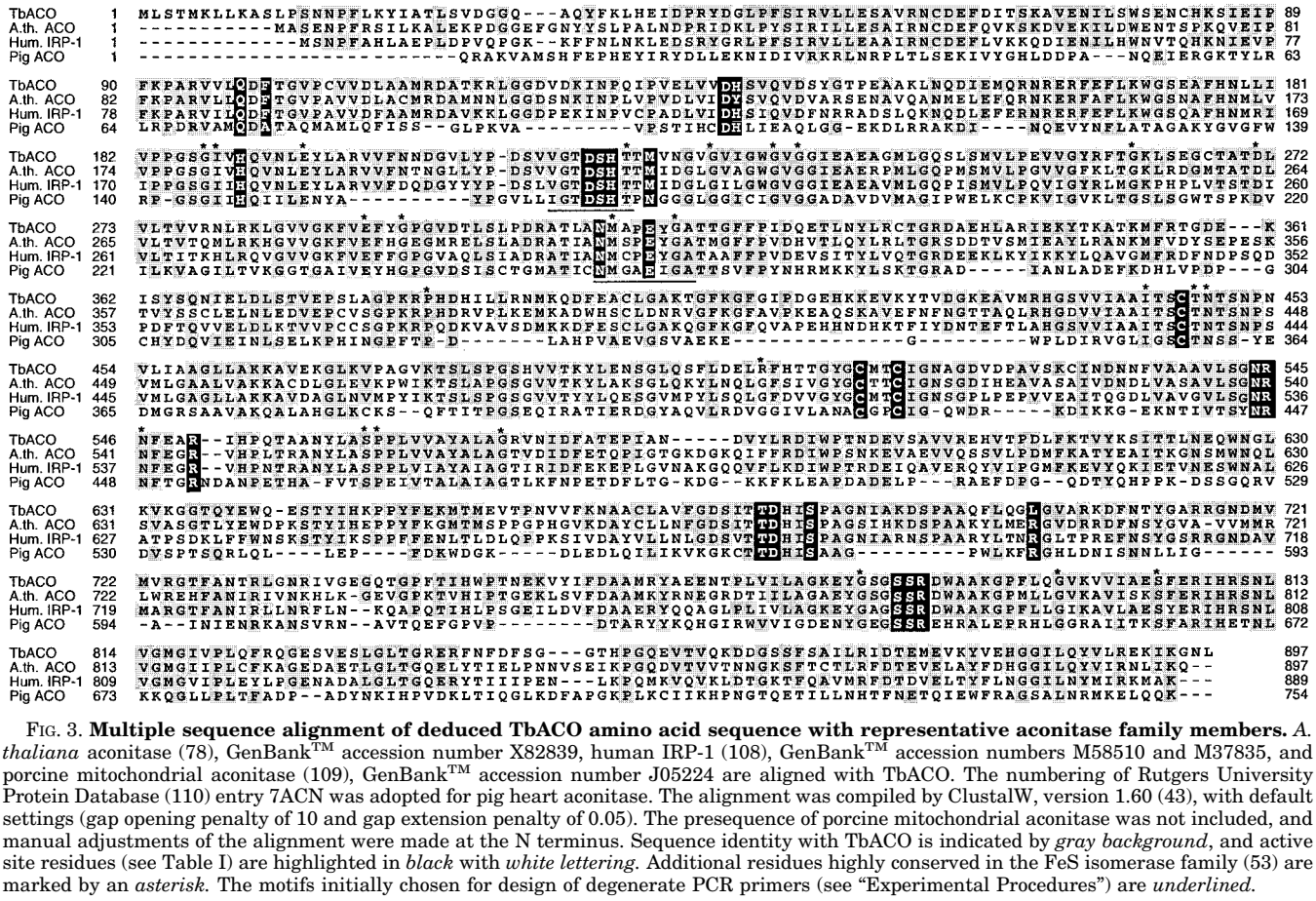

FIG. 3. **Multiple sequence alignment of deduced TbACO amino acid sequence with representative aconitase family members.** *A. thaliana* aconitase (78), GenBank™ accession number X82839, human IRP-1 (108), GenBank™ accession numbers M58510 and M37835, and porcine mitochondrial aconitase (109), GenBank™ accession number J05224 are aligned with TbACO. The numbering of Rutgers University Protein Database (110) entry 7ACN was adopted for pig heart aconitase. The alignment was compiled by ClustalW, version 1.60 (43), with default settings (gap opening penalty of 10 and gap extension penalty of 0.05). The presequence of porcine mitochondrial aconitase was not included, and manual adjustments of the alignment were made at the N terminus. Sequence identity with TbACO is indicated by *gray background*, and active site residues (see Table I) are highlighted in *black* with *white lettering.* Additional residues highly conserved in the FeS isomerase family (53) are marked by an *asterisk.* The motifs initially chosen for design of degenerate PCR primers (see "Experimental Procedures") are *underlined.*

ting procedure (40). Membranes were blocked overnight in TBST (25 mM Tris-HCl, pH 8, 150 mM NaCl, 0.1% (v/v) Tween 20), 5% (w/v) dried milk powder, incubated for 1 h with primary antibodies (1:1000) in TBST, 5% (w/v) dried milk powder, washed in TBST, and incubated with a second antibody conjugated to horseradish peroxidase or alkaline phosphatase for 1 h. Membranes were developed using the ECL detection kit (Amersham Pharmacia Biotech) or incubated in staining solution (0.41 mM NBT; 0.38 mM 5-bromo-4-chloro-3-indolyl phosphate; 4 mM $MgCl_2$; 0.1 M Tris-HCl, pH 9.5), respectively. Exposed films were scanned on a flat bed scanner (AGFA, model Arcus II), and the signals were quantified using NIH image software (version 1.60). Alternatively, the primary antibody was followed by a 1-h incubation with 1 μCi of ^{125}I-protein A (70–100 μCi/μg), several wash steps in TBST, and autoradiography on a PhosphorImager (Molecular Dynamics).

Digitonin Fractionation—Cell fractionation was essentially done as described by Häusler *et al.* (41). Aliquots of 2.5×10^7 procyclic cells were washed in 25 mM Tris-Cl, pH 7.8, 1 mM EDTA, 0.6 M sucrose, 1 mM DTT, 2 μg/ml leupeptin and were resuspended in 1.12 ml of the same buffer, and 125 μl of prediluted digitonin was added while mixing. After 2 min at 37 °C and 10 s on a Vortex mixer the cells were centrifuged at 12,000 × *g* at 4 °C for 10 min. The supernatant was concentrated by ultrafiltration using Microcon™ 30 (Amicon) before SDS-PAGE and immunoblotting of aliquots of both fractions.

Immunofluorescence—Short stumpy bloodstream forms were freshly isolated from infected mouse blood by centrifugation (22) and were stained with the mitochondrion-selective dye MitoTracker green FM™ (Molecular Probes) as described (42). Cells were then fixed in 3% (w/v) paraformaldehyde in PBS, permeabilized with 0.1% (v/v) Triton X-100 in PBS, and stained for 1 h with rabbit anti-TbACO antiserum or preimmune serum (Fig. 7*A*) diluted 1:10 in PBS, 1% (w/v) bovine serum albumin. Texas Red™-conjugated goat anti-rabbit IgG F(ab′)$_2$ fragments (Dianova) were used as secondary antibodies. Washed cells were mounted in VectaShield™ (Vector) on 3-aminopropyltriethoxy-silane-coated slides and were examined with a Zeiss Axiophot 2 microscope equipped with a Plan-Apochromat 63× objective (NA 1.4). Images were recorded with a cooled digital CCD camera (MicroMAX, Princeton Instruments).

Evolutionary Analysis—The multiple sequence alignments were generated with ClustalW, version 1.60 (43), and manual editing. The total length of the alignment comprises 1171 sites and is available upon request. To reconstruct phylogenetic trees based on the amino acid sequence alignment, the PUZZLE program (version 4.0) was applied (44, 45). As substitution model the substitution matrix BLOSUM 62 (46) was assumed. To account for rate heterogeneity a discrete Gamma model (47) with four categories was introduced, and the corresponding shape parameter was estimated. For each sequence we tested if the base composition deviates significantly from the average composition. The estimated shape parameter of the gamma distribution equals 1.17, thus indicating weak rate heterogeneity.

RESULTS

Cloning of an Aconitase Gene of T. brucei—Highly degenerate pools of PCR primers matching two conserved sequence motifs of the aconitase gene family were used to amplify genomic *T. brucei* DNA. Ten out of 31 clones derived from a PCR product of expected size contained the same 311-bp insert with an uninterrupted open reading frame exhibiting 74% protein sequence similarity to human IRP-1 and 75% similarity to *Arabidopsis thaliana* aconitase. No other aconitase family-related sequence was detected with this and other pairs of degenerate primers. The cloned 311-bp fragment was used to probe Southern blots of genomic DNA. Each restriction enzyme digest produced a single specific band with different mobility, indicating a single copy gene (Fig. 1). Low stringency hybridization conditions (40 °C below T_m) revealed only one additional sequence (marked with *asterisks* in Fig. 1) which was cloned from a phage library. The cross-hybridizing fragment did not exhibit any nucleotide sequence similarity to the aconitase gene family. Thus, the hybridization conditions used must have been sufficiently relaxed and sensitive for detection of *TbACO*-related genes. A restriction map of the *TbACO* locus was constructed from multiple digests, and a genomic 3.6-kb

*Sac*II-*Pst*I fragment was cloned (plasmid Tbaco1.1, see "Experimental Procedures" and Fig. 2) which contained a long open reading frame devoid of a stop codon. Therefore, a cDNA containing the missing C terminus was cloned by reverse transcriptase-PCR with nested *TbACO*-specific primers. An 800-bp internally primed cDNA was obtained. Therefore, the 3′-end of the gene was cloned by inverted PCR (see Fig. 2 and "Experimental Procedures"). The length of the 5′-UTR of the *TbACO* transcript was determined by a modified 5′-RACE strategy exploiting the conserved mini-exon sequence present at the 5′-end of all trypanosomal mRNAs. The sequence of three independent clones derived from the single PCR product showed that the mini-exon was added at a *trans*-splice site (AG dinucleotide) at position −100 relative to the first ATG codon. As expected for a canonical *trans*-splice site, several polypyrimidine stretches were found within 50 bp upstream of the AG.

The TbACO Protein Sequence—The open reading frame predicted a protein of 897 amino acids with a calculated molecular mass of 98,302 Da and a pI of 6.48. Both methionines at positions 1 and 5 are in sequence environments compatible with the requirements for translation initiation (48). Thus, use of the first ATG is assumed. Pairwise alignments of TbACO with other members of the aconitase family show a very high degree of amino acid identity and similarity with vertebrate IRPs and with plant aconitases (58/74% with human IRP-1; 61/75% with *A. thaliana* aconitase) extending over the entire length of the proteins. In contrast, mitochondrial aconitases of mammals or *S. cerevisiae* are significantly more distant (30% identity, 55% similarity). A multiple sequence alignment of TbACO with a representative member of each aconitase subfamily is shown in Fig. 3. From the crystal structure and mutation analysis of porcine mitochondrial aconitase, 24 residues were identified as important for coordination of the [4Fe-4S] cluster, for substrate recognition and catalysis, and for support of active site chains by hydrogen bonds (49–52). Table I lists the homologous positions in TbACO, showing that 21 of 24 positions are conserved. Asparagine 170 and alanine 74 of pig mitochondrial aconitase have been implicated in hydrogen bonding with other active site residues but are not conserved in the Fe-S isomerase family (53). In TbACO these positions are substituted by methionine (Met-222) and phenylalanine (Phe-100), respectively, like in mammalian IRPs and plant aconitases (see Fig. 3). Arginine 580 that appears to be a key residue for substrate binding in pig mitochondrial aconitase (52) has been replaced by leucine (Leu-702) in TbACO. This position is only substituted in two other aconitase sequences, that of *Legionella pneumophila* (54) and a hypothetical aconitase of *S. cerevisiae* (hACO) identified by genome sequencing (55). A multiple alignment of Frishman and Hentze (53) has identified 26 additional residues that are highly conserved in the Fe-S isomerase family (marked with an *asterisk* in Fig. 3). Of these, only one glycine (Gly-413 of pig mitochondrial aconitase) is substituted by arginine (Arg-504) in the TbACO sequence.

The high degree of sequence similarity of TbACO with IRPs, and the fact that trypanosomes represent the earliest branch of extant eukaryotes that harbor mitochondria (56), solicited a phylogenetic analysis. Sequences of 22 aconitases and IRPs available in data bases were aligned. As outgroup, sequences served 10 isopropylmalate isomerase and bacterial aconitase B group sequences that are significantly different. A PUZZLE tree based on 32 aligned sequences was reconstructed. For the 22 aconitase and IRP sequences a PUZZLE tree was computed and rooted according to the big tree (Fig. 4). The general topology of the tree is very similar to published trees of the aconitase family (53, 57, 58). TbACO is clearly separated from the mitochondrial aconitases. Within the IRP-like subfamily, TbACO,

TABLE I
Conservation of active site residues

Pig aconitase[a]	Assigned function[b]	TbACO[c]
Gln-72	Catalysis (49), substrate recognition (51)	Gln-98
Ala-74	Hydrogen bonds supporting active side chains (51)	*Phe-100*
Asp-100	Catalysis (49,51,52)	Asp-137
His-101	Catalysis (49–52)	His-138
His-147	Catalysis (49–52)	His-190
Asp-165	Catalysis (49–52)	Asp-217
Ser-166	Catalysis (49,50), substrate recognition (51)	Ser-218
His-167	Catalysis (49,51)	His-219
Asn-170	Formation of hydrogen bonded chain with N258, N446 (49,51)	*Met-222*
Asn-258	Interaction with FeS-cluster (51), catalysis (49)	Asn-310
Glu-262	Catalysis (49,51)	Glu-314
Cys-358	Ligation of FeS-cluster (49,51)	Cys-446
Cys-421	Ligation of FeS-cluster (49,51)	Cys-512
Cys-424	Ligation of FeS-cluster (49,51)	Cys-515
Asn-446	Interaction with FeS-cluster (51), catalysis (49)	Asn-544
Arg-447	Substrate recognition (51), catalysis (49,52)	Arg-545
Arg-452	Substrate recognition (51,52), catalysis (49)	Arg-550
Thr-567	Hydrogen bonds supporting active side chains (51)	Thr-680
Asp-568	Hydrogen bonds supporting active side chains (51)	Asp-681
Ser-571	Hydrogen bonds supporting active side chains (51)	Ser-684
Arg-580	Substrate recognition (51,52), catalysis (49)	*Leu-702*
Ser-642	Catalysis (49,51,52)	Ser-783
Ser-643	Substrate recognition (51), catalysis (49)	Ser-784
Arg-644	Substrate recognition (51), catalysis (49)	Arg-785

[a] Numbering of pig heart mitochondrial aconitase according to that used in Rutgers University Protein Database entry PDB code 7ACN.
[b] Inferred from crystal structures or site-directed mutagenesis.
[c] Homologous position in TbACO according to the alignment shown in Fig. 3. Substitutions are italicized.

plant aconitases, bacterial aconitases, and IRPs all branch from one node, and it is not possible to resolve the branching pattern any further. The statistical support for any particular topology linking TbACO to either the IRP cluster or the plant aconitase cluster is weak. This is congruent with recent evidence for an overestimation of the divergence of protists and crown eukaryotes, based on nuclear gene data, and the proposal of a "big bang" radiation of the various eukaryotic lineages (reviewed in Ref. 59).

Enzymatic Activity and Kinetic Properties of Recombinant TbACO—The complete open reading frame of *TbACO* was fused to a hexahistidine tag at the N terminus, and the fusion protein was expressed in *E. coli* and purified by affinity chromatography on a metal chelate resin (Fig. 5*A*). Aconitase activity increased linearly with the amount of recombinant protein and was maximal between pH 7 and 8 (not shown). The activity was dependent on loading of the protein with Fe^{2+} in the presence of DTT and was sensitive to oxygen (Table II), consistent with the presence of a labile [4Fe-4S] cluster (14, 36, 60). The conserved cysteine positions of TbACO ligating this putative iron-sulfur cluster (see Table I) were then substituted by serines by site-directed mutagenesis. Two recombinant mutant proteins (C446S and C512S/C515S) were purified and iron-loaded exactly as the wild type protein. As expected, no enzymatic activity could be detected (Table II and data not shown). The analogous mutations in human IRP-1 also abolished enzymatic activity (61, 62). This control provided unambiguous evidence that we had cloned an aconitase. The specific activity under V_{max} conditions was determined using >95% pure recombinant enzyme prepared by further purification on a MonoQ™ ion exchange column (Fig. 5*A*). The result was close to specific activities reported for bovine heart mitochondrial

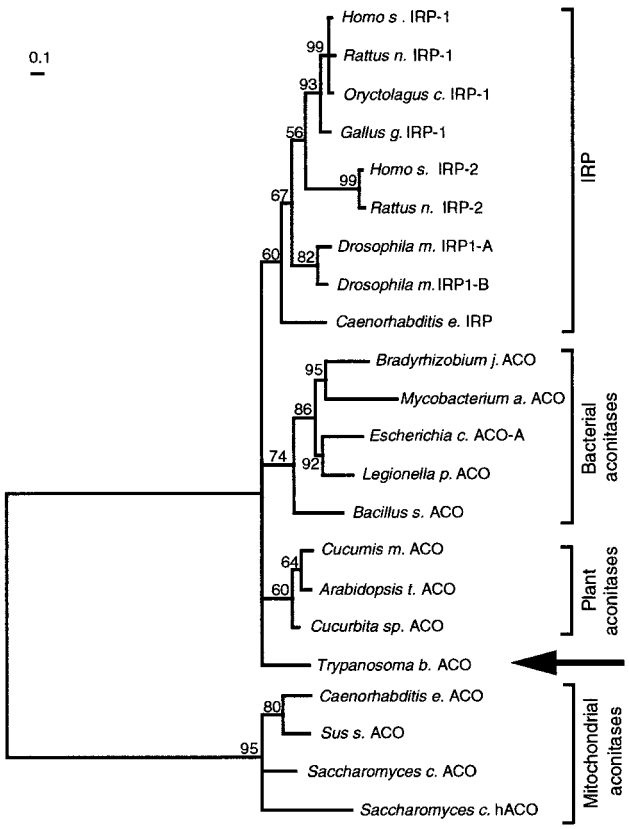

FIG. 4. **Phylogenetic tree of the aconitase family.** A PUZZLE tree was calculated for an alignment of 22 aconitases and IRPs (see "Experimental Procedures"). The tree was rooted with the information from a second tree that included 10 outgroup sequences (isopropylmalate isomerases and bacterial aconitase B group). The *numbers* along the edges indicate the support values (% of trees in a sample of 10,000 trees that show the same grouping (44)). The branch length is a measure of the number of substitutions (see scale). All sequences used for the alignment are available in public data bases. Accession numbers are listed in Refs. 55, 58, and 73.

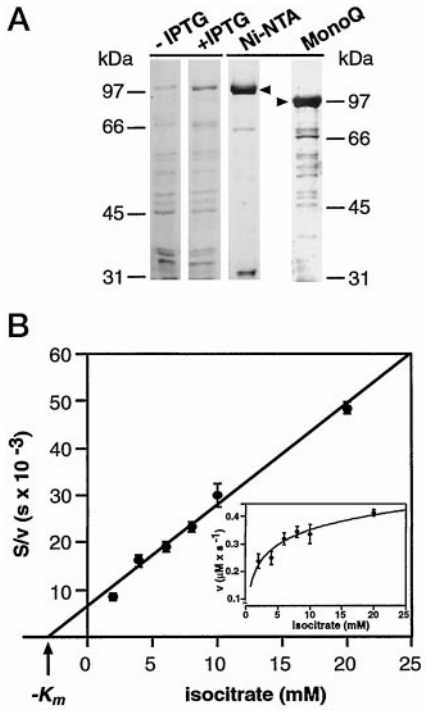

FIG. 5. **Kinetic analysis of recombinant TbACO.** Hexahistidine-tagged TbACO was expressed in *E. coli* and purified as described under "Experimental Procedures." *A*, Coomassie Brilliant Blue-stained (*1st to 3rd lanes*) or silver-stained (*4th lane*) 8% (w/v) SDS-PAGE: *1st lane*, bacterial lysate of the transformed *E. coli* M15rep4 (*−IPTG*); *2nd lane*, lysate prepared after induction of bacteria for 3 h with 1 mM IPTG at 25 °C (*+IPTG*); *3rd lane*, protein eluted from a nickel chelate affinity column (Ni^{2+}*-NTA*); *4th lane*, protein eluted from a second step MonoQ HR 5/5 ion exchange resin (MonoQ). Most of the faster migrating bands detected by silver staining (*4th lane*) are degradation products as indicated by immunoreactivity with anti-TbACO antibodies (not shown). TbACO eluted from Ni^{2+}-NTA was activated with Fe^{2+} and DTT under nitrogen atmosphere. Kinetic measurements with activated protein were performed with isocitrate as substrate, and formation of *cis*-aconitate was monitored spectroscopically at 240 nm. *B*, data representation as reciprocal [S/*v*]/[S] plot according to Hanes (38) with the original [*v*]/[S] (S, substrate concentration; *v*, reaction velocity) plot as *inset*. *Dots* indicate mean values, and *error bars* indicate standard deviations of a triplicate measurement. K_m = 2.9 mM and V_{max} = 10.6 μmol min^{-1} mg^{-1} were determined from the experiment shown. A mean of K_m = 3 ± 0.4 mM for the substrate isocitrate was calculated from five measurements with three independent protein preparations.

aconitase (30 μmol min^{-1} mg^{-1} (36, 52)), bovine IRP (34 μmol min^{-1} mg^{-1} (63)), and potato tuber mitochondrial aconitase (32 μmol min^{-1} mg^{-1} (64)). The Michaelis-Menten constant (K_m) for the substrate isocitrate was determined from reaction velocity plots and derived reciprocal Hanes plots as shown in Fig. 5*B*. The resulting K_m of 3 ± 0.4 mM is about 1 order of magnitude higher than published values for pig heart mitochondrial aconitase (65). This can be correlated with the substitution of an active site residue implicated in substrate binding (Leu-702 in TbACO substituting Arg-580 in pig mitochondrial aconitase, see Table I). In fact, an R580K mutant of pig mitochondrial aconitase (52) exhibits a 30-fold reduced K_m, nearly complete loss of tight substrate binding, and a 250–30,000-fold decreased activity, depending on the substrate. The ratio of the activities with isocitrate and citrate is 2.1 for the wild type but 11 for the R580K mutant (52). For TbACO, this ratio was 1.6 and the specific activity was close to that of wild type pig mitochondrial aconitase (Table II). This is even more surprising as the positive charge of the residue, which is thought to interact with the γ-carboxyl of substrates, is maintained in the R580K mutant of pig mitochondrial aconitase but replaced by the hydrophobic side chain of a leucine in TbACO. Thus, it seems that in TbACO a slightly different network of hydrogen bonds holds the substrate in place and substitutes for the proposed essential function of Arg-580 in the prototype aconitase structure (51, 66).

Differential Expression in the Life Cycle—A major *TbACO* transcript of 4.7 kb and a minor transcript of 4.2 kb were detected by Northern hybridization in three life cycle stages of *T. brucei*. The use of two polyadenylation sites was confirmed by mapping the cDNA with 3′-RACE-PCR (Fig. 2). No difference in total mRNA abundance was noted between stumpy bloodstream forms and procyclic forms, and the sum of the two transcripts was only slightly reduced in slender bloodstream forms (Fig. 6). Regulation appeared to be more prominent for the smaller mRNA; however, its contribution to the total amount of aconitase-specific mRNA was less than 30%. To investigate TbACO protein expression, antisera were produced in rats and rabbits by immunization with purified recombinant TbACO. Irrespective of the animal species and immunization procedure (see "Experimental Procedures"), one single polypeptide of 98 kDa was detected in procyclic whole cell lysates, in agreement with a predicted molecular mass of 98,302 Da. No signals were detected by the respective nonimmune or preimmune sera (Fig. 7*A*). TbACO expression was then compared in slender and stumpy bloodstream populations and in procyclic forms of the pleomorphic strain AnTat 1.1. The maximal amount of protein was detected in the procyclic stage (Fig. 7*B*). Expression in the slender bloodstream stage was less than 4% of the procyclic level, and stumpy populations were found to be

TABLE II
Enzymatic activity of recombinant purified TbACO

Enzyme	Activation Fe^{2+}/DTT	Anaerobic conditions	Reaction	Specific activity
				μmol min^{-1} *(mg protein)*$^{-1}$
rTbACO[a]	−	−	Isocitrate to cis-aconitate	Not detectable
rTbACO[a]	+	−	Isocitrate to *cis*-aconitate	2, variable
rTbACO[a]	+	+	Isocitrate to *cis*-aconitate	10.6[c]
C512S/C515S[a]	+	+	Isocitrate to *cis*-aconitate	Not detectable
rTbACO(MonoQ™)[b]	+	+	Isocitrate to *cis*-aconitate	13 ± 1.1[d]
rTbACO(MonoQ™)[b]	+	+	Citrate to *cis*-aconitate	8.3 ± 0.23[e]

[a] Expressed in *E. coli* and purified by affinity chromatography on Ni^{2+}-NTA as described under "Experimental Procedures."
[b] Further purification by ion exchange chromatography on MonoQ™ as described under "Experimental Procedures."
[c] Calculated from Fig. 5*B*.
[d] Mean ± S.D. of triplicate enzyme assay at 25 mM isocitrate.
[e] Mean ± S.D. (n = 4) at 60 mM citrate.

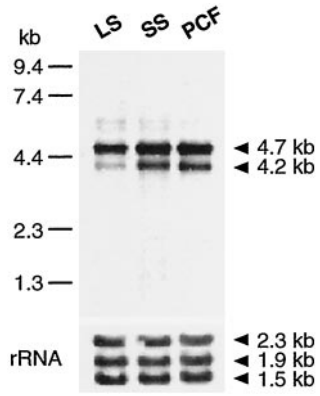

FIG. 6. **Developmental profile of *TbACO* mRNA expression.** A Northern blot with 5 μg of total RNA isolated from a long slender (*LS*) bloodstream form population, a short stumpy (*SS*) bloodstream form population, and cultured procyclic forms (*PCF*) of strain Antat1.1 was probed with a riboprobe derived from the coding region of *TbACO*. In the SS population, 90% of the cells expressed the stumpy cell marker NADH dehydrogenase, as assayed by cytochemical staining (6). Equal loading of samples was internally controlled by rehybridization of the blot with a rDNA probe detecting the 18 S rRNA and the α- and β-segments of 28 S rRNA. The relative abundance of the sum of the two *TbACO* transcripts marked with *arrowheads* was determined by densitometry and normalization to the rRNA signals (relative values are 1, 1.57, and 1.77 for LS, SS, and PCF, respectively). The size marker is an RNA ladder from Life Technologies, Inc.

intermediate. The same result was obtained with trypanosomes harvested from several independent rodent infections and upon probing with different antisera (not shown). The absolute TbACO abundance was estimated by comparison with standard dilutions of purified recombinant TbACO in the Western blot shown in Fig. 7*C* and calculated to be close to 160,000 molecules per procyclic cell. The fraction of stumpy forms in the predominantly slender or predominantly stumpy populations was determined by cytochemical staining for the stumpy marker activity NADH dehydrogenase (6) (see legend to Fig. 7). After correction, an estimation of 40,000 molecules per stumpy cell and 5000 molecules per slender cell was reached. In summary, developmental regulation of TbACO is more than 30-fold. This contrasts with a very minor change in mRNA expression. Thus, developmental control of expression must operate at the translational or post-translational level.

Subcellular Localization—The high sequence similarity of TbACO to IRPs, which are cytoplasmic regulatory proteins in mammalian cells, raised the question of its subcellular localization. TbACO was present but not enriched in a partially purified mitochondrial vesicle fraction prepared according to Ref. 67 (a kind gift of H. U. Goeringer, data not shown). This suggested multicompartmentalization of the protein. Therefore, procyclic trypanosomes were fractionated after differential permeabilization with digitonin. Based on different cholesterol content of the membranes, only the plasma membrane is permeabilized at low digitonin concentrations, whereas organellar membranes require higher concentrations (68–70). Phosphoglycerate kinase B and the mitochondrial heat shock protein HSP60 were used as markers for the cytosolic and mitochondrial fractions, respectively, as described before (41). Procyclic cells were incubated with increasing concentrations of digitonin, followed by centrifugal separation of soluble and particulate fractions. The amount of TbACO and of the marker proteins in each fraction was quantified by densitometric scanning of Western blots (Fig. 8, *A* and *B*). About 70% of total TbACO was released into the supernatant together with the cytosolic marker phosphoglycerate kinase B at 0.5 mg of digitonin per mg of cellular protein. The remaining part of TbACO appeared to be as resistant to solubilization as the mitochondrial matrix marker HSP60. To exclude the possibility that our antibodies cross-reacted with a different 98-kDa protein in one of the cellular compartments, TbACO was epitope-tagged at the C terminus with a short peptide derived from the yeast transposable element Ty1 (29). The tagged open reading frame was inserted into the trypanosomal expression vector pLew20 (28) and targeted to the ribosomal spacer region of the *T. brucei* genome by homologous recombination. The resulting procyclic cell line, which expressed about the same amount of tagged TbACO as wild type protein (not shown), was subjected to digitonin fractionation using the same conditions as for wild type procyclic forms. Western blots were probed with an epitope tag-specific monoclonal antibody (Fig. 8, *C* and *D*). About 70% of the tagged TbACO was released together with the cytosolic marker (phosphoglycerate kinase B) at low digitonin concentrations where the mitochondrial HSP60 was quantitatively retained in the pellet fraction. Together, these experiments proved that about 70% of TbACO was localized in the cytoplasm of procyclic *T. brucei*. Mitochondrial localization of the remaining 30% was suggested by the fractionation; however, the protease digestion control required to rule out nonspecific association of TbACO with the particulate fraction was technically difficult due to relative resistance of free TbACO to digestion. Instead, localization of TbACO to the single mitochondrion of trypanosomes was directly documented by immunofluorescence microscopy. In the stumpy stage, the mitochondrion has an easily discernible tubular structure extending over the entire length of the cell and can be visualized with the aldehyde-fixable membrane potential sensitive fluorescent dye MitoTracker™ Green FM (42). Upon immunofluorescent staining with three different TbACO-specific antisera, perfect colocalization of the antibody signal with the MitoTracker mitochondrial marker was observed in every cell (Fig. 9 and not shown). Double immunofluorescent staining with TbACO antibodies and antibodies detecting the mitochondrial matrix protein HSP60 also showed colocalization and confirmed antibody

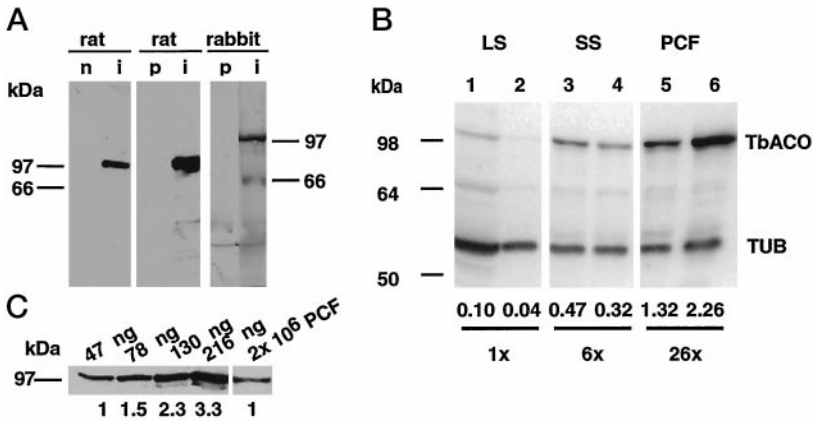

FIG. 7. **Developmental profile of TbACO protein expression.** Several antisera were raised in rats and rabbits against recombinant TbACO as detailed under "Experimental Procedures" to determine TbACO protein expression in different life cycle stages of *T. brucei*. *A*, Western blots documenting the specificity of three selected sera raised against a denatured 88-kDa rTbACO fragment (*rat 1*) or against the full-length 99-kDa rTbACO purified under native conditions (*rat 2, rabbit 1*). The equivalent of 5×10^6 procyclic trypanosomes per lane was run on 8% (w/v) SDS-PAGE and probed with nonimmune serum (*ni*, from a control animal of the same rat strain) or immune serum (*i*), or matched preimmune serum (*pi*) at the following dilutions: 1:500 for affinity purified sera from rat 1 and rat 2 and affinity purified controls; 1:100 for serum and control from rabbit 1. For detection, the ECL kit (*1st to 4th lanes*) or an alkaline phosphatase-catalyzed color reaction (*5th* and *6th lanes*) were used. *B*, lysates (two independent preparations for each developmental stage) of 5×10^6 long slender forms (*LS*, *lane 1*), 2×10^6 long slender forms (*LS*, *lane 2*), 2×10^6 short stumpy forms (*SS*, *lanes 3* and *4*), or 2×10^6 procyclic forms (*PCF*, *lanes 5* and *6*) of AnTat1.1 were size-fractionated by SDS-PAGE. The developmental stage of bloodstream form populations was verified with an established stumpy marker, NADH dehydrogenase, using cytochemical staining according to Vickerman (6). The slender populations contained <3% positive cells, and the stumpy populations contained >85% positive. TbACO was detected with purified rabbit 1 antibody (1:1000), and tubulin (*TUB*, internal control) was detected with rabbit anti-(*Dictyostelium* α-tubulin) serum (1:1000), followed by ^{125}I-protein A. Relative normalized intensities of TbACO bands as derived from PhosphorImager scans of ^{125}I and the fold regulation (average of $n = 2$) are indicated *below* the lanes. All samples were run on the same gel. *C,* absolute quantification of TbACO by Western blotting of a lysate from PCF together with dilutions of a highly purified rTbACO standard (see under "Experimental Procedures"). Affinity purified antibodies from rat 2 (1:500) and the ECL kit were used for detection. Relative intensity values derived from densitometry are indicated *below* the lanes. Linear regression analysis of the scanned standard signals was used for calculation.

access to the mitochondrial matrix under the given permeabilization conditions (data not shown). TbACO-specific cytoplasmic staining was weak, as expected from leakage of cytoplasmic protein during permeabilization necessary for detection of mitochondrial proteins (Fig. 9). In conclusion, TbACO has a dual subcellular localization in the cytosol and in the mitochondrion of *T. brucei*. Cytosolic and mitochondrial aconitase activity was then measured in lysates after preparative fractionation of procyclic trypanosomes with 0.5 mg of digitonin per mg of total protein. The fractionation was controlled with the marker proteins phosphoglycerate kinase B and HSP60, and the enzymatic assay showed that 78 ± 9% of the activity was in the cytoplasmic fraction and 21 ± 2% was associated with organelles. Thus, the subcellular distribution of aconitase activity was in agreement with the distribution of TbACO protein.

DISCUSSION

Mammalian cells have two aconitases encoded by separate nuclear genes: (*a*) the mitochondrial citric acid cycle enzyme and (*b*) a cytoplasmic aconitase, better known as the iron-regulatory protein (IRP-1) which acts as an iron sensor and post-transcriptional regulator and as a signal transducer for oxidative stress (71, 72). Since members of both aconitase subfamilies were identified in invertebrates, *e.g. Caenorhabditis elegans* and *Drosophila melanogaster* (73), specialization of mitochondrial and cytoplasmic aconitase functions seems to have occurred early during animal evolution. Here we report on a protozoan aconitase which belongs to the IRP-1 subfamily but localizes in the mitochondrion as well as in the cytoplasm. TbACO accounts for total aconitase activity in *T. brucei*. This was directly confirmed by enzyme assays in trypanosome lines with targeted disruption of both alleles of *TbACO*. In several independent Δ*aco::HYG*/Δ*aco::NEO* procyclic lines,[2] no aconitase activity could be detected (data not shown). The sensitivity of the enzymatic assay does not exclude a minor activity; however, three independent methods, PCR amplification with degenerate primers, low stringency Southern hybridizations, and Western blotting with several TbACO antisera (Fig. 1 and Fig. 7, and not shown), did not indicate a second aconitase or a second IRP-related gene in *T. brucei*.

The mitochondrial localization of about 30% of TbACO and the absence of a second aconitase indicate that TbACO functions in the citric acid cycle of *T. brucei*. To our knowledge, this is the first direct evidence that an IRP-like aconitase functions in mitochondrial metabolism in a eukaryote. The dual subcellular localization resembles the situation in plant tissues, where 50–90% of total aconitase activity or protein reside in the cytosol and function in the glyoxalate cycle (20, 21, 74, 75). Plant aconitase purified from cytosol and mitochondria is indistinguishable with respect to kinetic parameters, molecular mass (90–98 kDa), and the EPR spectrum (20, 64, 74–76). Furthermore, the molecular mass and the EPR spectrum of plant aconitase purified from mitochondria resemble mammalian IRP but not mammalian mitochondrial aconitase (64, 77). The three plant aconitase sequences available so far (21, 78) are very similar to IRPs and to TbACO but less related to the mitochondrial aconitase subfamily. Hence, it seems likely that the mitochondrial aconitase in plants is encoded by these IRP-related sequences, although direct evidence has yet to be provided. Particularly, it is unknown whether the cytosolic and mitochondrial plant aconitase isoforms, which are differentially regulated and chromatographically separable (20), derive from a single or distinct genes. The dual localization of the *T. brucei* aconitase, which is similar to plant aconitases (Fig. 3), suggests that cytosolic and mitochondrial IRP-related isoforms may indeed be encoded by one gene in plants.

As the first IRP-like sequence from a protist, the *TbACO* sequence has added valuable phylogenetic information with respect to evolution of the aconitase gene family (53, 57, 58, 79). The fact that *TbACO* forms a well supported clade together

[2] B. Fast and M. Boshart, unpublished data.

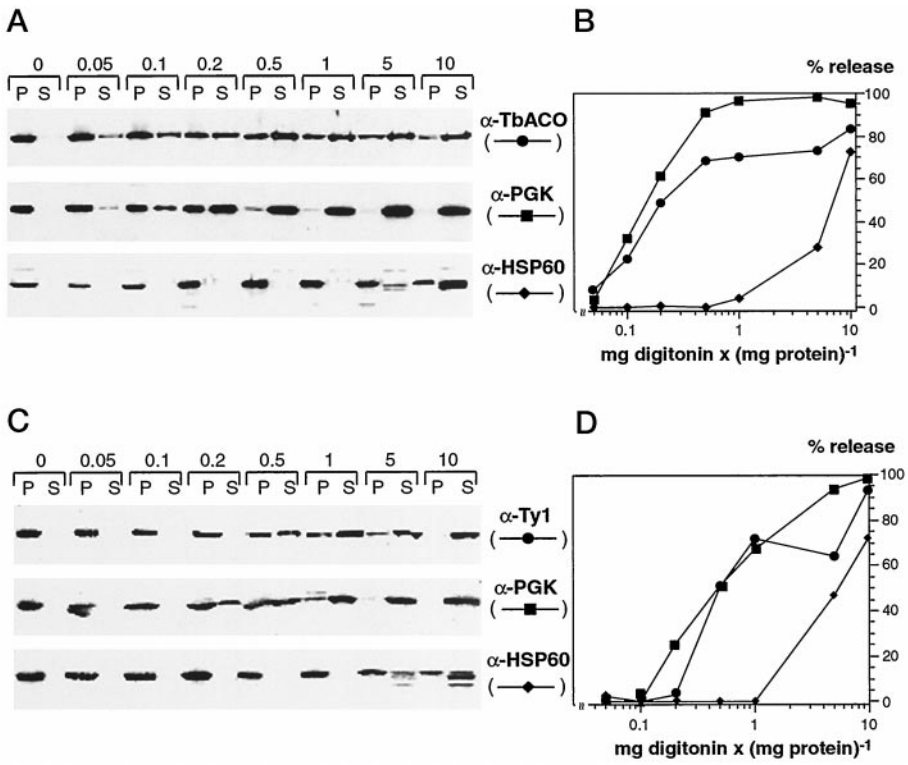

FIG. 8. **Subcellular localization (digitonin fractionation).** Procyclic trypanosomes were subjected to differential permeabilization by 0–10 mg of digitonin/mg of cellular protein (concentration indicated on *top* of the lanes in *A* and *C*, a different batch of digitonin was used for *C*) and were subsequently fractionated by centrifugation. Supernatant (*S*) and pellet (*P*) fractions were run on 8 or 10% (w/v) SDS-polyacrylamide gels and were analyzed by Western blotting using anti-phosphoglycerate kinase C serum (1:2000), anti-HSP60 serum (1:2000), affinity purified rat anti-TbACO serum (1:300), and anti-Ty1 monoclonal antibody (BB2 culture supernatant, 1:50) as indicated. Phosphoglycerate kinase B (*PGK-B,* detected by anti-phosphoglycerate kinase C serum) served as cytosolic marker and mitochondrial heat shock protein HSP60 served as mitochondrial marker (41). *A* and *B*, AnTat1.1 wild type procyclic trypanosomes (2.5×10^6 or 5×10^6 cells (for *HSP60* only) per lane). *C* and *D*, transgenic MiTat1.4 procyclic trypanosomes stably expressing an epitope (*Ty1*)-tagged TbACO. Western blots are shown in *A* and *C,* and the corresponding quantitative data obtained by densitometric scanning are displayed in *B* and *D*. The released fraction (*% release*) is calculated by dividing the amount of specific protein in the supernatant by the total amount of specific protein in supernatant and pellet of the respective sample.

with animal IRPs, plant aconitases, and bacterial aconitases of the *E. coli acoA* type, clearly separated from mitochondrial aconitases of yeast and animals (Fig. 4), strengthens the argument for the existence of aconitase paralogues before the separation of eubacteria from eukaryotes. The mitochondrial localization of TbACO and the branching of IRP, TbACO, and bacterial aconitases from one node support the view that the ancestor of the regulatory protein IRP was an enzyme of mitochondrial energy metabolism which most likely was acquired from a proteobacterial endosymbiont. It seems that members of the IRP-like and of the classical mitochondrial aconitase subfamilies both can function in more than one subcellular compartment. In *S. cerevisiae,* which does not harbor an IRP-related gene in its genome (80), the mitochondrial aconitase is also present in the cytosol where it participates in the glyoxalate cycle (81). In trypanosomes, the single IRP-like aconitase is present in the mitochondrion and in the cytosol, and in plants, IRP-related aconitases seem to function in mitochondrial metabolism as well as in the cytosolic step of the glyoxalate cycle (20, 21, 75). Animals may have kept or acquired members of both aconitase subfamilies during evolution and restricted them to one subcellular compartment in order to specialize them for different tasks in the mitochondrion and in the cytosol.

The distribution of one gene product between different subcellular compartments can be achieved by a variety of mechanisms, most of which lead to alternative transcription and/or translation initiation sites or alternative mRNA processing (reviewed in Ref. 82). In the case of TbACO, there is only one defined 5′-end of the mRNA and two closely spaced potential AUG codons at positions 1 and 5. It is difficult to imagine alternative translation initiation at these positions to include a mitochondrial import presequence in a fraction of the synthesized protein. Furthermore, the N-terminal sequence of TbACO does not form an amphipathic helix and does not predict a classical mitochondrial targeting signal. The mechanisms for protein import in trypanosomes seem to be largely conserved (41, 83–86); however, a second class of much shorter, typically 9 amino acid long presequences that resemble hydrogenosomal import sequences has been identified (87). At least one imported protein (cytochrome c_1) lacks a presequence (88), and a nonconservative import pathway has been suggested (86). Mitochondrial and cytoplasmic TbACO were never resolved as double band upon PAGE of *T. brucei* lysates, and hence, there is no evidence for cleavage of a leader sequence. However, cleavage of both mitochondrial and cytosolic mature protein as shown for *S. cerevisiae* fumarase FUM1 (89) cannot be excluded. All fumarase molecules synthesized in yeast are processed by the mitochondrial matrix protease, but nevertheless most of the enzyme (80–90%) ends up in the cytosol. An aborted translocation process has been suggested to be responsible for the dual mitochondrial and cytoplasmic localization of *S. cerevisiae* fumarase FUM1 (89). It should be noted that the 9 amino acid presequence of *T. brucei* dihydrolipoamide dehydrogenase which is sufficient for import (85, 87) is cleaved off in both bloodstream and procyclic forms, although the protein is not present in the mitochondrion of slender bloodstream forms (90–93). We suggest that multicompartmentalization of TbACO is due to inefficient targeting or an aborted translocation mechanism, possibly associated with a weak import signal

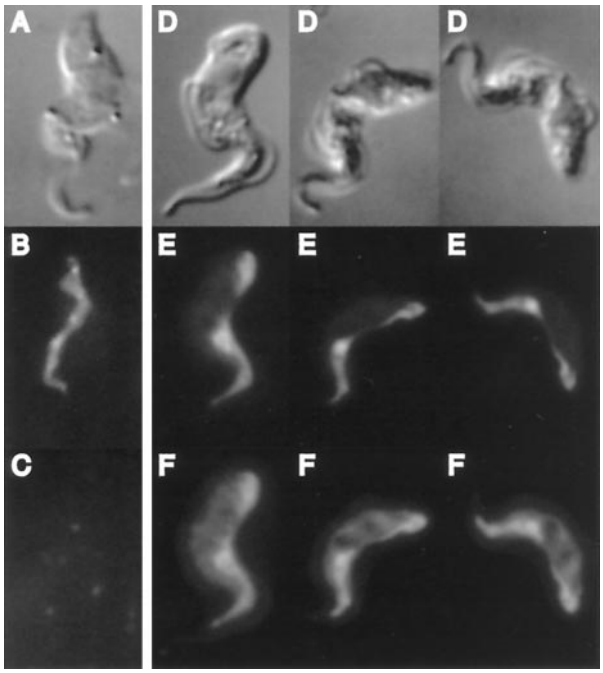

FIG. 9. **Subcellular localization (immunofluorescence).** Short stumpy stage bloodstream forms were stained with the mitochondrion-selective dye MitoTracker Green FM™, fixed, permeabilized with 0.1% (v/v) Triton X-100, and incubated with rabbit preimmune serum (*A–C*) or anti-TbACO antiserum (*D-F*) and Texas Red™-conjugated goat anti-rabbit $F(ab')_2$ fragments. *A* and *D*, phase contrast. *B* and *E*, MitoTracker Green FM™ fluorescence observed with fluorescein isothiocyanate filter set. *C* and *F*, Texas Red™ fluorescence observed with red filter set. Three representative cells are displayed for *D–F*.

deviating from the presequence consensus features.

Why do trypanosomes have a cytoplasmic IRP-like aconitase? First, it is possible that the protein serves a gene regulatory function similar to mammalian IRP. Recently, the *Bacillus subtilis* IRP-like aconitase has been shown to bind to mammalian IREs (94). The sequence motif DLVIDH-IQV implicated in RNA binding of IRP (95) is nearly conserved in TbACO (three conservative substitutions); however, no sequence-specific binding of the mammalian IRE consensus RNA sequence to recombinant purified TbACO could be detected.[2] The putative trypanosomal target RNA sequence may deviate, and thus a regulatory role can only be addressed genetically. We have investigated expression and regulation of one possible target, the trypanosomal transferrin receptor, and found no change of its expression or regulation in cells carrying a targeted deletion of *TbACO* (96). Second, we have considered the possibility that TbACO serves as cytoplasmic iron store. In fact, the IRP-related aconitase of *L. pneumophila* is the major iron-containing protein in that organism (54). However, a calculation based on the iron uptake rate of trypanosomes (97) showed that TbACO should contribute less than 10% to the total iron content of proliferating slender bloodstream forms. Given the abundance of cytoplasmic TbACO, particularly in the procyclic stage, a metabolic function seems the most likely. In plant tissues, cytoplasmic aconitase is developmentally regulated with a dramatic increase during seed and pollen maturation and during germination, reflecting glyoxalate cycle activity (reviewed in Ref. 19). Evidence for a glyoxalate cycle in stationary promastigotes (probably metacyclic forms) of the trypanosomatid *Leishmania* has been reported (98, 99). Although key enzymes of the glyoxalate cycle have not been detected in procyclic forms of *T. brucei* in culture,[3] a functional glyoxalate cycle may be operative and important at some later stage in the insect vector, where utilization of storage lipids may compensate for temporary shortage of nutrients. We are currently testing this hypothesis by tsetse fly passage of *TbACO* knock out strains.

Citric acid cycle activities and certain respiratory chain activities are turned on in the stumpy bloodstream stage of *T. brucei* as a preadaptation to the tsetse midgut environment, where rapid differentiation to the procyclic stage is essential for survival (5, 8). The developmental profile of TbACO expression fully accounts for the previously reported changes of total aconitase activity (5, 7) and parallels the developmental changes in energy metabolism in the trypanosomal life cycle (1, 2). More than 30-fold developmental regulation of TbACO contrasts with only a minor change of mRNA abundance, indicating a translational or post-translational mechanism. The only other citric acid cycle enzyme that has been cloned so far, malate dehydrogenase, seems to be regulated in a similar fashion (100). We anticipate that a common translational or post-translational mechanism may coordinately up-regulate citric acid cycle activities upon differentiation. Whereas numerous examples suggest a predominance of regulation at the level of differential mRNA stability in trypanosomatids (101, 102), only a handful of examples of translational or post-translational regulation have been reported (103–107).

Acknowledgments—M. van den Bogaard and C. Modes contributed to the subcellular localization and protein purification, respectively. We thank P. Michels for the phosphoglycerate kinase antiserum; U. Goeringer for a partially purified mitochondrial vesicle fraction; P. Bastin and K. Gull for the BB2 hybridoma; G. Gerisch for α-tubulin antiserum; E. Vassella for a Northern filter; and H. Lauble and P. Overath for critical reading of the manuscript.

REFERENCES

1. Vickerman, K. (1985) *Br. Med. Bull.* **41,** 105–114
2. Fairlamb, A. H., and Opperdoes, F. R. (1986) in *Carbohydrate Metabolism in Cultured Cells* (Morgan, M. J., ed) pp. 183–224, Plenum Publishing Corp., New York
3. Opperdoes, F. R. (1987) *Annu. Rev. Microbiol.* **41,** 127–151
4. Clayton, C. E., and Michels, P. (1996) *Parasitol. Today* **12,** 465–471
5. Durieux, P. O., Schütz, P., Brun, R., and Köhler, P. (1991) *Mol. Biochem. Parasitol.* **45,** 19–28
6. Vickerman, K. (1965) *Nature* **208,** 762–766
7. Overath, P., Czichos, J., and Haas, C. (1986) *Eur. J. Biochem.* **160,** 175–182
8. Priest, J. W., and Hajduk, S. L. (1994) *J. Bioenerg. Biomembr.* **26,** 179–191
9. Reuner, B., Vassella, E., Yutzy, B., and Boshart, M. (1997) *Mol. Biochem. Parasitol.* **90,** 269–280
10. Vassella, E., Reuner, B., Yutzy, B., and Boshart, M. (1997) *J. Cell Sci.* **110,** 2661–2671
11. Brun, R., and Schonenberger, M. (1981) *Z. Parasitenk.* **66,** 17–24
12. Matthews, K. R., and Gull, K. (1997) *J. Cell Sci.* **110,** 2609–2618
13. Beinert, H., Kennedy, M. C., and Stout, C. D. (1996) *Chem. Rev.* **96,** 2335–2373
14. Kent, T. A., Dreyer, J. L., Kennedy, M. C., Huynh, B. H., Emptage, M. H., Beinert, H., and Munck, E. (1982) *Proc. Natl. Acad. Sci. U. S. A.* **79,** 1096–1100
15. Theil, E. C. (1994) *Biochem. J.* **304,** 1–11
16. Rouault, T. A., Klausner, R. D., and Harford, J. B. (1996) *Translational Control*, pp. 335–362, Cold Spring Harbor Laboratory, Cold Spring Harbor, NY
17. Kühn, L. C., and Hentze, M. W. (1992) *J. Inorg. Biochem.* **47,** 183–195
18. Hentze, M. W., and Kühn, L. C. (1996) *Proc. Natl. Acad. Sci. U. S. A.* **93,** 8175–8182
19. Escher, C. L., and Widmer, F. (1997) *Biol. Chem. Hoppe-Seyler* **378,** 803–813
20. De Bellis, L., Hayashi, M., Nishimura, M., and Alpi, A. (1995) *Planta* **195,** 464–468
21. Hayashi, M., De Bellis, L., Alpi, A., and Nishimura, M. (1995) *Plant Cell Physiol.* **36,** 669–680
22. Vassella, E., and Boshart, M. (1996) *Mol. Biochem. Parasitol.* **82,** 91–105
23. Cross, G. A. M. (1975) *Parasitology* **71,** 393–417
24. Hirumi, H., and Hirumi, K. (1989) *J. Parasitol.* **75,** 985–989
25. Brun, R., and Schonenberger, M. (1979) *Acta Trop.* **36,** 289–292
26. Lanham, S. M., and Godfrey, D. G. (1970) *Exp. Parasitol.* **28,** 521–534
27. Carruthers, V. B., van der Ploeg, L. H. T., and Cross, G. A. M. (1993) *Nucleic Acids Res.* **21,** 2537–2538
28. Wirtz, E., Hoek, M., and Cross, G. A. M. (1998) *Nucleic Acids Res.* **26,** 4626–4634
29. Bastin, P., Bagherzadeh, A., Matthews, K. R., and Gull, K. (1996) *Mol. Biochem. Parasitol.* **77,** 235–239
30. Boshart, M., Weih, F., Nichols, M., and Schütz, G. (1991) *Cell* **66,** 849–859
31. Mizobuchi, M., and Frohman, L. A. (1992) *BioTechniques* **12,** 350–354
32. Ausubel, F. M., Brent, R., Kingston, R. E., Moore, D. D., Seidman, J. G., Smith,

[3] F. Opperdoes, personal communication.

J. A., and Struhl, K. (1987) *Current Protocols in Molecular Biology*, John Wiley & Sons, Inc., New York
33. White, T. C., Rudenko, G., and Borst, P. (1986) *Nucleic Acids Res.* **14,** 9471–9489
34. Villarejo, M. R., and Zabin, I. (1974) *J. Bacteriol.* **120,** 466–474
35. Murakami, K., and Yoshino, M. (1997) *Biochem. Mol. Biol. Int.* **41,** 481–486
36. Kennedy, M. C., Emptage, M. H., Dreyer, J. L., and Beinert, H. (1983) *J. Biol. Chem.* **258,** 11098–11105
37. Henson, C. P., and Cleland, W. W. (1967) *J. Biol. Chem.* **242,** 3833–3838
38. Hanes, C. S. (1932) *Biochem. J.* **26,** 1406–1421
39. Olmsted, J. B. (1981) *J. Biol. Chem.* **256,** 11955–11957
40. Towbin, H., Staehelin, T., and Gordon, J. (1979) *Proc. Natl. Acad. Sci. U. S. A.* **76,** 4350–4354
41. Häusler, T., Stierhof, Y.-D., Wirtz, E., and Clayton, C. (1996) *J. Cell Biol.* **132,** 311–324
42. Vassella, E., Straesser, K., and Boshart, M. (1997) *Mol. Biochem. Parasitol.* **90,** 381–385
43. Thompson, J. D., Higgins, D. G., and Gibson, T. J. (1994) *Nucleic Acids Res.* **22,** 4673–4680
44. Strimmer, K., and von Haeseler, A. (1996) *Mol. Biol. Evol.* **13,** 964–969
45. Strimmer, K., Goldman, N., and Vonhaeseler, A. (1997) *Mol. Biol. Evol.* **14,** 210–211
46. Henikoff, S., and Henikoff, J. G. (1992) *Proc. Natl. Acad. Sci. U. S. A.* **89,** 10915–10919
47. Yang, Z. (1994) *J. Mol. Evol.* **39,** 306–314
48. Kozak, M. (1983) *Microbiol. Rev.* **47,** 1–45
49. Robbins, A. H., and Stout, C. D. (1989) *Proteins* **5,** 289–312
50. Robbins, A. H., and Stout, C. D. (1989) *Proc. Natl. Acad. Sci. U. S. A.* **86,** 3639–3643
51. Lauble, H., Kennedy, M. C., Beinert, H., and Stout, C. D. (1992) *Biochemistry* **31,** 2735–2748
52. Zheng, L., Kennedy, M. C., Beinert, H., and Zalkin, H. (1992) *J. Biol. Chem.* **267,** 7895–7903
53. Frishman, D., and Hentze, M. W. (1996) *Eur. J. Biochem.* **239,** 197–200
54. Mengaud, J. M., and Horwitz, M. A. (1993) *J. Bacteriol.* **175,** 5666–5676
55. Purnelle, B., Coster, F., and Goffeau, A. (1994) *Yeast* **10,** 1235–1249
56. Sogin, M. L. (1991) *Curr. Opin. Gen. & Dev.* **1,** 457–463
57. Gruer, M. J., Artymiuk, P. J., and Guest, J. R. (1997) *Trends Biochem. Sci.* **22,** 3–6
58. Irvin, S. D., and Bhattacharjee, J. K. (1998) *J. Mol. Evol.* **46,** 401–408
59. Gray, M. W., Burger, G., and Lang, F. (1998) *Science* **283,** 1476–1481
60. Beinert, H., Emptage, M. H., Dreyer, J. L., Scott, R. A., Hahn, J. E., Hodgson, K. O., and Thomson, A. J. (1983) *Proc. Natl. Acad. Sci. U. S. A.* **80,** 393–396
61. Philpott, C. C., Haile, D., Rouault, T. A., and Klausner, R. D. (1993) *J. Biol. Chem.* **268,** 17655–17658
62. Hirling, H., Henderson, B. R., and Kühn, L. C. (1994) *EMBO J.* **13,** 453–461
63. Kennedy, M. C., Mende-Mueller, L., Blondin, G. A., and Beinert, H. (1992) *Proc. Natl. Acad. Sci. U. S. A.* **89,** 11730–11734
64. Verniquet, F., Gaillard, J., Neuburger, M., and Douce, R. (1991) *Biochem. J.* **276,** 643–648
65. Pickworth Glusker, J. (1971) *Enzymes* **5,** 413–439
66. Lauble, H., and Stout, C. D. (1995) *Proteins* **22,** 1–11
67. Harris, M. E., Moore, D. R., and Hajduk, S. L. (1990) *J. Biol. Chem.* **265,** 11368–11376
68. Schulz, I. (1990) *Methods Enzymol.* **192,** 280–300
69. Sommer, J. M., Cheng, Q.-L., Keller, G.-A., and Wang, C. C. (1992) *Mol. Biol. Cell* **3,** 749–759
70. Zhang, J. W., Luckey, C., and Lazarow, P. B. (1993) *Mol. Biol. Cell* **4,** 1351–1359
71. Hentze, M. W. (1996) *Trends Biochem. Sci.* **21,** 282–283
72. Rouault, T. A., and Klausner, R. D. (1996) *Trends Biochem. Sci.* **21,** 174–177
73. Muckenthaler, M., Gunkel, N., Frishman, D., Cyrklaff, A., Tomancak, P., and Hentze, M. W. (1998) *Eur. J. Biochem.* **254,** 230–237
74. Brouquisse, R., Nishimura, M., Gaillard, J., and Douce, R. (1987) *Plant Physiol.* (*Bethesda*) **84,** 1402–1407
75. Courtois Verniquet, F., and Douce, R. (1993) *Biochem. J.* **294,** 103–107
76. De Bellis, L., Tsugeki, R., Alpi, A., and Nishimura, M. (1993) *Physiol. Plant.* **88,** 485–492
77. Jordanov, J., Courtois-Verniquet, F., Neuburger, M., and Douce, R. (1992) *J. Biol. Chem.* **267,** 16775–16778
78. Peyret, P., Perez, P., and Alric, M. (1995) *J. Biol. Chem.* **270,** 8131–8137
79. Zhou, Y. H., and Ragan, M. A. (1995) *Plant Mol. Biol.* **28,** 635–646
80. Mewes, H. W., Albermann, K., Bahr, M., Frishman, D., Gleissner, A., Hani, J., Heumann, K., Kleine, K., Maierl, A., Oliver, S. G., Pfeiffer, F., and Zollner, A. (1997) *Nature* **387,** (suppl.) 7–8
81. Gangloff, S. P., Marguet, D., and Lauquin, G. J. M. (1990) *Mol. Cell. Biol.* **10,** 3551–3561
82. Danpure, C. J. (1995) *Trends Cell Biol.* **5,** 230–238
83. Clayton, C., Hausler, T., and Blattner, J. (1995) *Microbiol. Rev.* **59,** 325–344
84. Priest, J. W., and Hajduk, S. L. (1995) *Biochim. Biophys. Acta* **1269,** 201–204
85. Hauser, R., Pypaert, M., Häusler, T., Horn, E. K., and Schneider, A. (1996) *J. Cell Sci.* **109,** 517–523
86. Priest, J. W., and Hajduk, S. L. (1996) *J. Biol. Chem.* **271,** 20060–20069
87. Häusler, T., Stierhof, Y. D., Blattner, J., and Clayton, C. (1997) *Eur. J. Cell Biol.* **73,** 240–251
88. Priest, J. W., Wood, Z. A., and Hajduk, S. L. (1993) *Biochim. Biophys. Acta* **1144,** 229–231
89. Stein, I., Peleg, Y., Even-Ram, S., and Pines, O. (1994) *Mol. Cell. Biol.* **14,** 4770–4778
90. Jackman, S. A., Hough, D. W., Stevenson, D. J., and Opperdoes, F. R. (1990) *Eur. J. Biochem.* **193,** 91–95
91. Else, A. J., Hough, D. W., and Danson, M. J. (1993) *Eur. J. Biochem.* **212,** 423–429
92. Else, A. J., Clarke, J. F., Willis, A., Jackman, S. A., Hough, D. W., and Danson, M. J. (1994) *Mol. Biochem. Parasitol.* **64,** 233–239
93. Tyler, K. M., Matthews, K. R., and Gull, K. (1997) *Proc. R. Soc. Lond. Ser. B Biol. Sci.* **264,** 1481–1490
94. Alén, C., and Sonenshein, A. L. (1999) *Proc. Natl. Acad. Sci. U. S. A.* **96,** 10412–10417
95. Basilion, J. P., Rouault, T. A., Massinople, C. M., Klausner, R. D., and Burgess, W. H. (1994) *Proc. Natl. Acad. Sci. U. S. A.* **91,** 574–578
96. Fast, B., Krempa, K., Boshart, M., and Steverding, D. (1999) *Biochem. J.* **342,** 691–696
97. Steverding, D. (1998) *Parasitol. Res.* **84,** 59–62
98. Keegan, F. P., and Blum, J. J. (1993) *J. Euk. Microbiol.* **40,** 730–732
99. Blum, J. J. (1994) *J. Bioenerg. Biomembr.* **26,** 147–155
100. Anderson, S. A., Carter, V., and Parsons, M. (1998) *Exp. Parasitol.* **89,** 63–70
101. Clayton, C. (1992) *Prog. Nucleic Acids Res. Mol. Biol.* **43,** 37–66
102. Vanhamme, L., and Pays, E. (1995) *Microbiol. Rev.* **59,** 223–240
103. Torri, A. F., Bertrand, K. I., and Hajduk, S. L. (1993) *Mol. Biochem. Parasitol.* **57,** 305–316
104. Gale, M., Jr., Carter, V., and Parsons, M. (1994) *J. Biol. Chem.* **269,** 31659–31665
105. Priest, J. W., and Hajduk, S. L. (1994) *Mol. Biochem. Parasitol.* **65,** 291–304
106. Schürch, N., Furger, A., Kurath, U., and Roditi, I. (1997) *Mol. Biochem. Parasitol.* **89,** 109–121
107. Hotz, H. R., Hartmann, C., Huober, K., Hug, M., and Clayton, C. (1997) *Nucleic Acids Res.* **25,** 3017–3025
108. Rouault, T. A., Tang, C. K., Kaptain, S., Burgess, W. H., Haile, D. J., Samaniego, F., McBride, O. W., Harford, J. B., and Klausner, R. D. (1990) *Proc. Natl. Acad. Sci. U. S. A.* **87,** 7958–7962
109. Zheng, L., Andrews, P. C., Hermodson, M. A., Dixon, J. E., and Zalkin, H. (1990) *J. Biol. Chem.* **265,** 2814–2821
110. Bernstein, F. C., Koetzle, T. F., Williams, G. J., Meyer, E. F., Jr., Brice, M. D., Rodgers, J. R., Kennard, O., Shimanouchi, T., and Tasumi, M. (1977) *Eur. J. Biochem.* **80,** 319–324